J|A|C|S
ARTICLES
Published on Web 05/18/2007

A Magnetism-Assisted Chemical Vapor Deposition Method To Produce Branched or Iron-Encapsulated Carbon Nanotubes

Dacheng Wei, Yunqi Liu,* Lingchao Cao, Lei Fu, Xianglong Li, Yu Wang, and Gui Yu

Contribution from the Beijing National Laboratory for Molecular Sciences, Institute of Chemistry, Chinese Academy of Sciences, Beijing 100080, P.R. China

Received January 11, 2007; E-mail: liuyq@mail.iccas.ac.cn

Abstract: A magnetism-assisted chemical vapor deposition method was developed to synthesize branched or iron-encapsulated carbon nanotubes. In the process, the external magnetic field can promote the coalescence or division of the catalyst particles, causing the formation of branched or encapsulated nanostructures. This finding will extend the understanding of the chemical vapor deposition method in a magnetic field and promote the applications of branched or encapsulated nanostructures.

Introduction

Carbon nanotubes (CNTs), as one hopeful nanomaterial for nanoelectronics, exhibit widespread applications for their outstanding properties,[1−4] and these applications can be largely expanded, improved, or altered by forming branched or encapsulated architectures. For example, the magnetic properties of CNTs have been investigated for more than 10 years,[5−8] however the applications of CNTs in magnetism are still limited in success due to their poor magnetic properties. Thus, many researchers follow another approach by encapsulating magnetic metals into CNTs to realize the applications of CNTs in magnetism, such as high-density magnetic storage, magnetic inks, drug delivery, magnetic resonance imaging, etc.[9−13] Moreover, the branched CNTs show rectifying[14,15] and ballistic switching[16,17] properties while the pristine CNTs do not. For these reasons and the absence of a common synthetic method, much attention has been focused on the synthesis of branched or encapsulated CNTs in recent years.[18−24]

One of the most used methods for synthesizing CNTs is the chemical vapor deposition (CVD) process,[25,26] which is also a general method for producing other one-dimensional nanomaterials.[27,28] This process can be dramatically influenced by the external field, consequently causing a variation of the architecture of the products. For example, in an electronic field[29] or gas flow field,[30,31] CNTs will grow and form an array parallel to the field direction. Wei et al.[32] found that in a fluctuant flow field branched junctions could form due to the coalescence of catalyst. Therefore, the external field offers a feasible way to control the CVD process. In this article, we introduce another normal field, a magnetic field, into the CVD process, and then CNTs with branched or iron encapsulated structures are synthesized by the magnetism-assisted CVD method.

Experimental Section

The experimental setup is illustrated in Scheme 1. Branched or iron encapsulated CNTs were synthesized via a magnetism-assisted CVD method by pyrolysis of iron(II) phthalocyanine (FePc). In a typical

(1) Frank, S.; Poncharal, P.; Wang, Z. L.; Heer, W. A. *Science* **1998**, *280*, 1744−1746.
(2) Tans, S. J.; Verschueren, A. R. M.; Dekker, C. *Nature* **1998**, *393*, 49−52.
(3) Yao, Z.; Postma, H. W. C.; Balents, L.; Dekker, C. *Nature* **1999**, *402*, 273−276.
(4) Chen, Z. H.; Appenzeller, J.; Lin, Y. M.; Sippel-Oakley, J.; Rinzler, A. G.; Tang, J.; Wind, S.; Solomon, P.; Avouris, P. *Science* **2006**, *311*, 1735−1736.
(5) Tian, W. D.; Datta, S. *Phys. Rev. B* **1994**, *49*, 5097−5100.
(6) Bachtold, A.; Strunk, C.; Salvetat, J. P.; Bonard, J. M.; Forra, L.; Nussbaumer, T.; Schanenberger, C. *Nature* **1999**, *397*, 673−675.
(7) Roche, S.; Saito, R. *Phys. Rev. Lett.* **2001**, *87*, 246803.
(8) Zaric, S.; Ostojic, G. N.; Kono, J.; Shaver, J.; Moore, V. C.; Strano, M. S.; Hauge, R. H.; Smalley, R. E.; Wei, X. *Science* **2004**, *304*, 1129−1131.
(9) Mühl, T.; Elefant, D.; Graff, A.; Kozhuharova, R.; Leonhardt, A. *Appl. Phys. Lett.* **2003**, *93*, 7984−7986.
(10) Mönch, I.; Meye, A.; Leonhardt, A.; Krämer, K.; Kozhuharova, R.; Gemming, T.; Wirth, M. P.; Büchner, B. *J. Magn. Magn. Mater.* **2005**, *290−291*, 276−278.
(11) Su, Y. C.; Hsu, W. K. *Appl. Phys. Lett.* **2005**, *87*, 233122.
(12) Urías, F. L.; Sandoval, E. M.; Reyes, M. R.; Romero, A. H.; Terrones, M.; López, J. L. M. *Phys. Rev. Lett.* **2005**, *94*, 216102.
(13) Wei, B.; Shima, M.; Pati, R.; Nayak, S. K.; Singh, D. J.; Ma, R. Z.; Li, Y. B.; Bando, Y.; Nasu, S.; Ajayan, P. M. *Small* **2006**, *2*, 804−809.
(14) Papadopoulos, C.; Rakitin, A.; Li, J.; Vedeneev, A. S.; Xu, J. M. *Phys. Rev. Lett.* **2000**, *85*, 3476.
(15) Andriotis, A. N.; Menon, M.; Srivastava, D.; Chernozatonskii, L. *Phys. Rev. Lett.* **2001**, *87*, 066802.
(16) Andriotis, A. N.; Menon, M.; Srivastava, D.; Chernozatonskii, L. *Appl. Phys. Lett.* **2001**, *79*, 266−268.
(17) Bandaru, P. R.; Daraio, C.; Jin, S.; Rao, A. M. *Nat. Mater.* **2005**, *4*, 663−666.
(18) Elias, A. L.; et al. *Nano Lett.* **2005**, *5*, 467−672.
(19) Che, R.; Peng, L. M.; Chen, Q.; Duan, X. F.; Gu, Z. N. *Appl. Phys. Lett.* **2003**, *82*, 3319−3321.
(20) Bao, J.; Tie, C.; Xu, Z.; Suo, Z.; Zhou, Q.; Hong, J. *Adv. Mater.* **2002**, *14*, 1483−1486.
(21) Li, J.; Papadopoulos, C.; Xu, J. *Nature* **1999**, *402*, 253−254.
(22) Meng, G.; Jung, Y. J.; Cao, A.; Vajtai, R.; Ajayan, P. M. *Proc. Natl. Acad. Sci. U.S.A.* **2005**, *102*, 7074−7078.
(23) Gothard, N.; Daraio, C.; Gaillard, J.; Zidan, R.; Jin, S.; Rao, A. M. *Nano Lett.* **2004**, *4*, 213−217.
(24) Terrones, M.; Banhart, F.; Grobert, N.; Charlier, J. C.; Terrones, H.; Ajayan, P. M. *Phys. Rev. Lett.* **2002**, *89*, 075505.
(25) Raty, J. Y.; Gygi, F.; Galli, G. *Phys. Rev. Lett.* **2005**, *95*, 096103.
(26) Lin, M.; Tan, J. P. Y.; Boothroyd, C.; Loh, K. P.; Tok, E. S.; Foo, Y. L. *Nano Lett.* **2006**, *6*, 449−452.
(27) Wagner, R. S.; Ellis, W. C. *Appl. Phys. Lett.* **1964**, *4*, 89−91.
(28) Hu, J.; Odom, T. W.; Lieber, C. M. *Acc. Chem. Res.* **1999**, *32*, 435−445.
(29) Ural, A.; Li, Y. M.; Dai, H. J. *Appl. Phys. Lett.* **2002**, *81*, 3464−3466.
(30) Huang, S. M.; Cai, X. Y.; Du, C. S.; Liu, J. *J. Phys. Chem. B* **2003**, *107*, 13251−13254.
(31) Hong, B. H.; Lee, J. Y.; Beetz, T.; Zhu, Y.; Kim, P.; Kim, K. S. *J. Am. Chem. Soc.* **2005**, *127*, 15336−15337.

10.1021/ja0702465 CCC: $37.00

Scheme 1. Presentation of the Experimental Setup

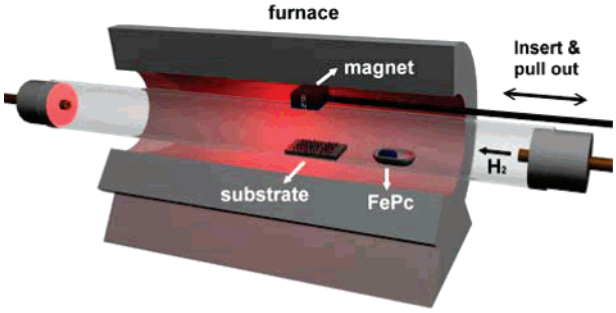

experiment, hydrogen gas (99.99%) was used as carrier gas through a quartz tube at a steady flux of 40 sccm. As the furnace temperature reached 950 °C, a quartz boat with 0.05 g of FePc (Acros Organics Corp., Morris Plains, NJ), which was used as both carbon source for CNT growth and iron source for catalyst and encapsulated material, was placed in the region of 550 °C, and then FePc was evaporated from the boat and pyrolyzed in the high-temperature region downstream, where a silicon wafer with a 500 nm oxidation layer was placed as a substrate for the CNT growth. The reaction lasted for 12 min. During the reaction, we inserted a Sm_2Co_{17} magnet into the reaction place of the furnace for 10 s and then pull it out, and this process was repeated every 30 s. The magnetic induction was about 0.2 T, and the magnetic induction gradient was about 50 $mT \cdot cm^{-1}$ around the surface of the magnet. The inserted magnet was located above or beside the substrate; thus, the magnetic field was parallel or vertical to the CNT growth direction. To avoid the demagnetization of the magnet at high temperature, a piece of wet cloth was covered on the magnet, thus allowing the temperature of the magnet to remain below 100 °C. After the reaction, the product was annealed at 950 °C for 5 min to provide sufficient thermal energy to make CNTs into perfectly crystalline structures. Finally, the reactor was cooled to room temperature under the H_2 ambient after the growth.

The samples were characterized by scanning electron microscopy (SEM, Hitachi S-4300, operated at 15 kV), transmission electron microscopy (TEM, Hitachi-2010, operated at 200 kV), and X-ray photoelectron spectroscopy (XPS, ESCA Lab220I-XL). The substrate with product was split from the middle, and then the profile of CNT arrays was examined by SEM. The magnetic measurements were performed in a vibrating-sample magnetometer (Lakeshore 7307) at 298 K in normal pressure.

Results and Discussion

Figure 1 shows SEM images of the products produced by introducing a magnetic field vertical (product: CNT⊥) or parallel (product: CNT∥) to CNT growth direction. They are arrays of well-aligned CNTs perpendicular to the substrate. Iron particles are on the base of CNTs adhering to the substrate as catalyst, indicating that the growth of CNTs follows a base growth mode. From TEM images, we can find there are three types of CNTs in both of the products, which are branched CNTs (Figure 2a), iron-encapsulated CNTs (Figure 2b), and iron-encapsulated branched CNTs (Figure 2c). However, the yield of each type is different. More branched junctions are observed in CNT⊥ (about 60%) than in CNT∥ (about 10%), while higher contents of iron-encapsulated CNTs are found in CNT∥ (about 70%) than in CNT⊥ (about 15%). To confirm this result, these products were examined by XPS (Figure 3). The peak at 284.8 eV corresponds to C 1s of the graphitelike carbon atoms of the tube walls, while the peaks at 707.2 and 720.1 eV corresponds

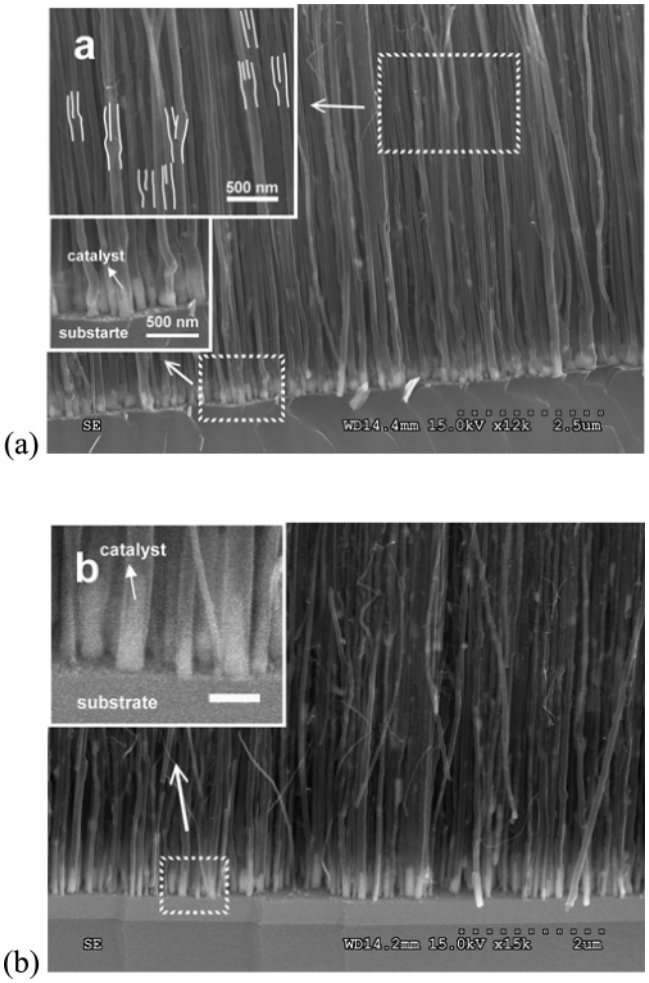

Figure 1. SEM images of arrays of CNTs produced by introducing a magnetic field vertical (a) or parallel (b) to the CNT growth direction. The insets are the higher magnified images of the areas indicated by dashed frames, and the branched junctions are contoured in white lines for clarity.

to Fe(0) 2p3/2 and Fe(0) 2p1/2 of the encapsulated iron particles. The small peaks centered at 398.6 and 532.8 eV correspond to N 1s and O 1s, and the small amount of N and O comes from the reactant FePc and the surface absorption of oxygen gas, respectively. The wide range XPS spectrum of CNT∥ shows the predominant presence of carbon (89.6 at. %), and iron (1.9 at. %). Compared with CNT⊥ (C 96.0 at. %, Fe 0.6 at. %), the atomic composition of CNT∥ reveals a prominent increase of iron, indicating there are more encapsulated iron particles in CNT∥. The detailed structures of a "Y" junction and an iron-encapsulated CNT are examined by high-resolution TEM (HRTEM) as shown in Figure 4. Both images indicate that the CNTs are multiwalled and perfectly graphitized with the interlayer separation of 3.4 Å. The center of the branched CNT is hollow with graphitic sheets gradually bent parallel to the corner, while at the corner of two branches the graphitic layers are abruptly bent and many defects exist in this area due to the presence of nonhexagonal carbon rings in the graphitic sheet. Most encapsulated particles are well-crystallized with a clearly resolved interlayer separation of 0.20 nm, corresponding to the (110) crystal plane of α-iron, and the selected-area electron diffraction (SAED) patterns (Figure S1 in the Supporting Information) also confirm this result.

(32) Wei, D. C.; Liu, Y. Q.; Cao, L. C.; Fu, L.; Li, X. L.; Wang, Y.; Yu, G.; Zhu, D. B. *Nano Lett.* **2006**, *6*, 186−192.

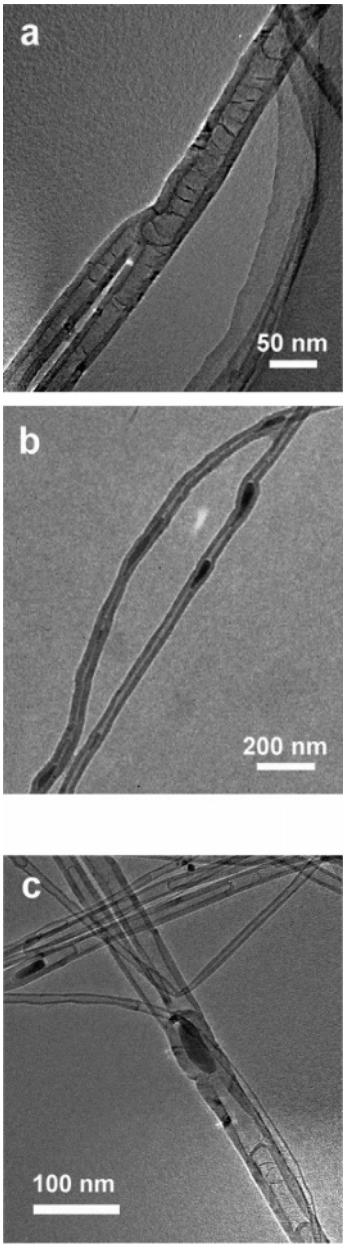

Figure 2. TEM images of a branched CNT (a), iron-encapsulated CNTs (b), and an iron-encapsulated branched CNT (c).

In viewing of the configuration of the products, a coalescence or division mechanism of catalyst particles could be proposed for the formation of branched junctions or encapsulated structures, respectively (Scheme 2). Almost all branched junctions have a similar configuration. The stems are located below the branches, with catalyst on the base adhering to the substrate, so the branches should grow before the growth of the stems. Around the junction area, the diameter of the stem usually corresponds to the aggregation of the branches, thus indicating the catalyst for the stem has a similar size with the aggregation of the catalysts for the branches, because the diameter of CNTs are defined by the size of the catalyst.[33] Therefore, the coalescence of catalysts should take place in the process, and then branched junctions form accompanied by the growth of the stem from the coalescent catalyst. The splitting of catalyst

(33) Cheung, C. L.; Kurtz, A.; Park, H. K.; Lieber, C. M. *J. Phys. Chem. B* **2002**, *106*, 2429−2433.

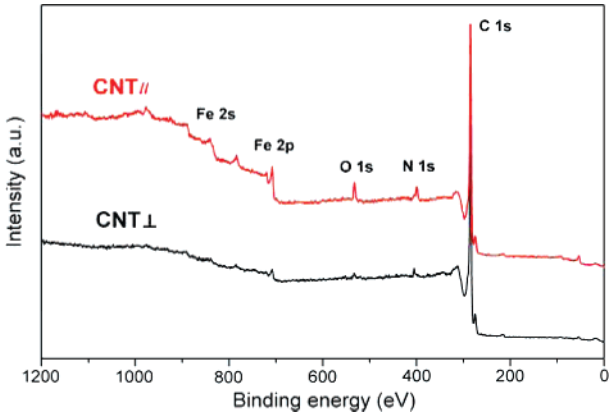

Figure 3. Wide survey XPS spectra of CNT arrays produced by introducing a magnetic field vertical (black line) or parallel (red line) to the CNT growth direction.

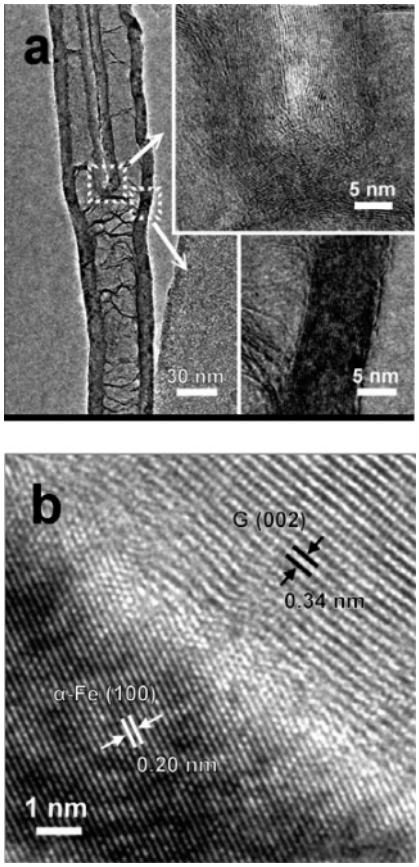

Figure 4. HRTEM images of a branched CNT (a) and an iron-encapsulated CNT (b). The inset of (a) shows the higher magnified images of the areas indicated by dashed frames.

particles, which can also induce the formation of branched junctions, could be eliminated, because the catalyst particles are only detected at the base of the stems. Moreover, some "V"-shaped CNTs are detected in the products, in which the catalyst just coalesces without the growth of the stems. The iron-encapsulated CNTs also have a similar configuration. Iron particles are located in the straight cavity of the CNTs successionally, and one particle always remains at the base of the CNTs as catalyst. It is not possible that encapsulation comes from the diffusion of iron atoms through the CNT walls but from division of catalyst particles, because the CNT walls are

Scheme 2. Presentation of the Formation of Branched or Iron-Encapsulated CNTs[a]

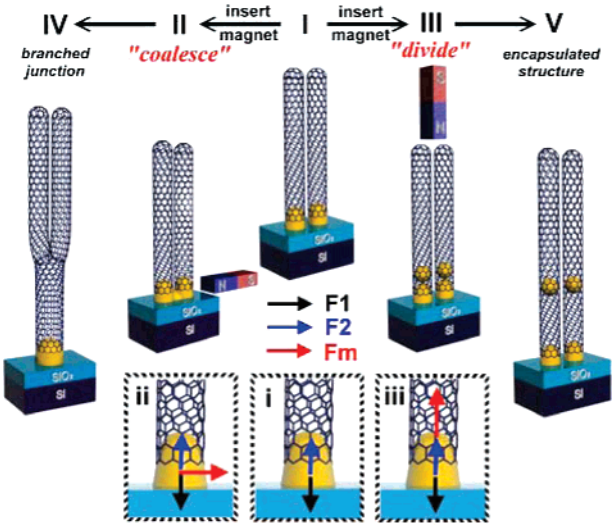

[a] The lower insets of i−iii show the forces applied to the catalyst in the stages of I−III, Respectively. F_1 indicates the adhesion force of the substrate, F_2 indicates the adhesion force of the CNT for the capillary effect, and F_m indicates the magnetic force applied to the catalyst.

perfectly closed with only one peristome which is filled by catalyst.

The magnetic field plays a pivotal role in the coalescence or division process. In normal cases, if the CNTs grow in a steady environment, the catalyst particles will remain in a stable state, and then one-dimensional CNTs with few branched junctions or encapsulated iron particles grow as Dai et al. reported.[34,35] However, as Helveg et al. detected in situ by HRTEM, the catalyst particles were elongated into CNTs for the capillary effect and suddenly contracted due to the surface tension in the growth.[36] Although the vapor−liquid−solid process, which causes the formation of CNTs, dominates the growth, some other factors also exist and influence the growth of CNTs, causing the formation of CNTs with various morphologies. Therefore, by pyrolysis of FePc, CNTs with curved, helical, coiled, double-helical, and tube-within-tube shapes could be observed in the products.[37] In fact, many factors can also induce the formation of branched CNTs in a CVD process, like the flow fluctuation,[32] the dopant of sulfur,[38] copper,[39] or titanium[40] in the catalyst, etc.; similarly, many routes have been reported to synthesize encapsulated CNTs in a CVD process.[41−43] However, in our cases, these factors for branching or encapsulation are avoided, because the amount of branched junctions and encapsulated

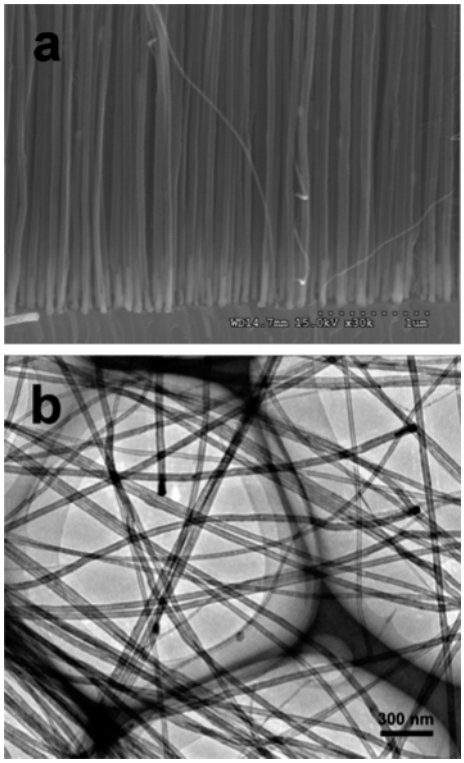

Figure 5. SEM image (a) and TEM image (b) of CNTs produced in a normal CVD process by pyrolysis of FePc without the magnetic field.

particles is very little if we pyrolyze FePc without the magnetic field. Figure 5 shows the SEM and TEM images of the product. Therefore, in our case, the branching or encapsulation would come from another factor. The catalyst particles are inclined to coalesce to reduce the surface tension but usually remain in an uncoalescent state for the interval of neighboring catalyst particles, the obstacle of CNT walls, the adhesion of the substrate, etc.[32] Meanwhile, the catalyst particles are inclined to fill into CNTs for the capillary effect[44−46] but usually remain on the base of CNTs for the adhesion of the substrate.[35] Due to these two opposite factors, the catalyst particles tend to divide and consequently encapsulate into CNTs; however, the division is prohibited by surface tension. So in a steady environment, the catalyst particles remain in a stable state without coalescence and division, and then the products are mainly straight CNTs without branches or encapsulated particles (Figure 5).[34,35] However, magnetic metals like Fe, Co, and Ni are usually used as the catalysts for CNT growth, and they remain magnetic even in the liquid state at high temperture.[47] So if we insert a magnet, a magnetic force (F_m) is applied to iron particles, which can be calculated by

$$F_m = m\chi H\mathrm{grad}(H)$$

where m is the mass, χ is the susceptibility, H is the magnetic field strength, and grad(H) is the magnetic field strength gradient. So, in the gradient magnetic field of the magnet, a magnetic force can be applied to the small catalyst particles.

(34) Huang, S. M.; Dai, L. M.; Mau, A. W. H. *J. Phys. Chem. B* **1999**, *103*, 4223−4227.
(35) Fan, S.; Chapline, M. G.; Franklin, N. R.; Tombler, T. W.; Cassell, A. M.; Dai, H. J. *Science* **1999**, *283*, 512−514.
(36) Helveg, S.; Cartes, C. L.; Sehested, J.; Hansen, P. L.; Clausen, B. S.; Nielsen, J. R.; Pedersen, R. F. A.; Norskov, J. K. *Nature* **2004**, *427*, 426−429.
(37) Huang, S. M.; Dai, L. M. *J. Nanopart. Res.* **2002**, *4*, 145.
(38) Satishkumar, B. C.; Thoma, P. J.; Govindaraj, A.; Rao, C. N. R. *Appl. Phys. Lett.* **2000**, *77*, 2530−2532.
(39) Gan, B.; Ahn, J.; Zhang, Q.; Rusli Yoon, S. F.; Yu, J.; Huang, Q. F.; Chew, K.; Li, W. Z. *Chem. Phys. Lett.* **2001**, *333*, 23−28.
(40) Gothard, N.; Daraio, C.; Gaillard, J.; Zidan, R.; Jin, S.; Rao, A. M. *Nano Lett.* **2004**, *4*, 213−217.
(41) Che, R.; Peng, L.-M.; Chen, Q.; Duan, X. F.; Zou, B. S.; Gu, Z. N. *Chem. Phys. Lett.* **2003**, *375*, 59−64.
(42) Che, R.; Peng, L.-M.; Chen, Q.; Duan, X. F.; Gu, Z. N. *Appl. Phys. Lett.* **2003**, *82*, 3319−3321.
(43) Kim, N. S.; Lee, Y. T.; Park, J.; Han, J. B.; Choi, Y. S.; Choi, S. Y.; Choo, J. *J. Phys. Chem. B* **2003**, *107*, 9249−9255.
(44) Dujardin, E.; Ebbesen, T. W.; Hiura, H.; Tanigaki, K. *Science* **1994**, *265*, 1850−1851.
(45) Ajayan, P. M.; Iijima, S. *Nature* **1993**, *361*, 333−334.
(46) Ajayan, P. M.; Ebbesen, T. W.; Ichihashi, T.; Iijima, S.; Tanigaki, K.; Hiura, H. *Nature* **1993**, *362*, 522−525.
(47) Urbain, G.; Ubelacker, E. *Adv. Phys.* **1967**, *16*, 429.

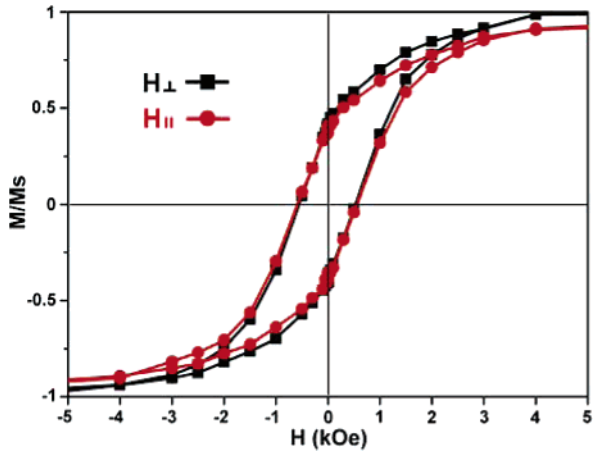

Figure 6. Magnetic hysteresis loops of an iron-encapsulated CNT array in room temperature.

Xie et al. also observed the existence of a magnetic force due to liquid iron particles in the growth of carbon nanofiber.[48] Accompanying the insertion of the magnet, F_m will largely vary, causing the breakdown of the steady state of the CNT growth. If the magnet is inserted beside the substrate, F_m, which is perpendicular to the CNTs, can cause the catalysts to overcome the obstacles to coalesce, and then branched CNTs form due to the continuous growth of CNT from the coalescent catalyst. If the magnet is inserted on top of the substrate, F_m, which is parallel to the CNTs, can apply to the catalyst an impetus to divide and fill into CNTs and then iron encapsulated CNTs form. Actually, because the magnetic field around the magnet is a nonparallel field, F_m with both directions can be applied to the catalysts in the insertion process of magnet, although one direction dominates. So both types of CNTs can be observed in the products, and one type dominates. And, if the catalyst particles go through both a coalescence process and a division process, iron-encapsulated branched CNTs will form as shown in Figure 2c.

The content of encapsulated iron particles can be influenced by the intensity of the magnetic field. Here, three types of magnets were used in the magnetism-assisted CVD process, which were an AlNiCo magnet (0.02 T), a Sm_2Co_{17} magnet (0.2 T), and an AlFeB magnet (0.4 T). The SEM and TEM images of the products (CNT|) are shown in Figure S2 (Supporting Information). We can find that using the AlNiCo magnet, only a few iron particles are encapsulated, while a larger amount of encapsulated particles can be observed if the Sm_2Co_{17} or AlFeB magnet is used. Therefore, a higher intensity of magnetic field will benefit the iron encapsulation. Moreover, due to the limitation of the experimental conductions, in our research, the magnetic field is introduced into the CVD process by a magnet, which is cooled and protected by a piece of wet cloth to avoid the demagnetization at high temperature. Although the effect of the magnetic field on the CVD process is obvious under our conditions, the effect would be more obvious and controllable if we use coils around the growth zone to generate magnetic field, because the coils can provide a larger and more stable magnetic field and the magnetic field can be easily controlled by the electrical current of the coils.

To investigate magnetic properties, we measured an iron-encapsulated CNT array by a vibrating-sample magnetometer at room temperature in normal pressure. Figure 6 shows the magnetic hysteresis loops for the directions perpendicular or parallel to the CNTs, respectively. The saturation magnetization/unit area is about 21 μemu·mm^{-2}, and the remanence is about 8 μemu·mm^{-2}. Compared with pure bulk iron, an enhancement of coercivity is observed. The coercivities perpendicular (Hc⊥) and parallel (Hc|) to the CNTs are measured about 531 and 556 Oe, respectively, much larger than that of bulk iron ($H_c \approx$ 0.15 Oe). This is attributed to the small size effect of magnetic particles[49] and the protection of the CNT walls, because the CNT walls confine the encapsulated particles to a nanoscale space, prohibit the oxidation of iron particles, and then ensure a long-term stability of the ferromagnetic core.

Conclusions

In summary, we developed a simple and effective method to synthesize branched or iron-encapsulated CNTs through a new route by introducing a magnetic field into a CVD process. We investigated the branching or encapsulating process, and a mechanism of magnetic field promoted coalescence or division of catalyst particles is proposed. By encapsulation of the CNTs, the coercivity of iron is largely enhanced, showing wide potential applications in high-density magnetic storage, magnetic inks, ferrofluids, drug delivery, etc. Moreover, this method can not only be used to produce branched or encapsulated CNTs but also has the potential to produce branched or encapsulated nanostructures made of other materials, which also use magnetic catalysts. This finding will extend the understanding of the CVD method in a magnetic field and promote the applications of branched or encapsulated nanostructures.

Acknowledgment. This work was supported by the Major State Basic Research Development Program, the National Natural Science Foundation of China (Grants 90206049, 20472089, 20421101, 20573115, 50673093, and 60671047), and the Chinese Academy of Sciences.

Supporting Information Available: Figures S1 (the SAED patterns of encapsulated iron particle) and S2 (SEM and TEM images of CNTs produced by inserting an AlNiCo, Sm_2Co_{17}, or AlFeB magnet) and complete ref 18. This material is available free of charge via the Internet at http://pubs.acs.org.

JA0702465

(48) Sun, L. F.; Liu, Z. Q.; Ma, X. C.; Tang, D. S.; Zhou, W. Y.; Zou, X. P.; Li, Y. B.; Lin, J. Y.; Tan, K. L.; Xie, S. S. *Chem. Phys. Lett.* **2001**, *336*, 392−396.

(49) Frenkel, J.; Dorfman, J. *Nature* **1930**, *126*, 274−275.